

1985

NASA/ASEE SUMMER FACULTY RESEARCH FELLOWSHIP PROGRAM

MARSHALL SPACE FLIGHT CENTER
THE UNIVERSITY OF ALABAMA IN HUNTSVILLE

ON THE DETERMINATION OF THE ORIGIN OF LINEAR
ANOMALY IN THE MACROSTRUCTURE OF VPPA WELDED
2219-T87 ALUMINUM ALLOY

Prepared by:	Wartan A. Jemian
Academic Rank:	Professor
University:	Auburn University
Department:	Mechanical and Materials Engineering
NASA/MSFC:	
Laboratory:	Materials and Processes Lab
Division:	Processes Engineering
Branch:	Metal Processes
MSFC Counterpart:	Arthur Nunes
Date:	August 16, 1985
Contract Number:	NGT 01-008-021 The University of Alabama in Huntsville

FINAL REPORT
ON THE DETERMINATION OF THE ORIGIN
OF LINEAR ANOMALY IN THE MACROSTRUCTURE OF
VPPA WELDED 2219-T87 ALUMINUM ALLOY

by Warton A. Jemian, Ph. D.
Professor of Mechanical Engineering and Materials Engineering
Auburn University
Alabama

16 August 1985

ABSTRACT

The objective of this summer research was to determine the cause and significance of the weld radiograph enigma, which is a linear anomaly in the features of the x-ray film. By observing features on available radiographs and in studying published reports of similar features it was possible to conclude that there are many manifestations of the enigma, and that they are all specific features of fine structure in radiographs due to natural processes connected with welding and to specific X-ray absorption and diffraction phenomena. These processes include the thermal distribution and liquid metal flow in welding, the development of microstructure, morphology, second phase particles and porosity due to the solidification process and to the pattern of residual stresses after the weld metal has cooled to the ambient temperature. Microdensitometer traces were made across weld radiographs of standard and enigmatic types. Similar patterns were produced by computer simulation. These show that the enigma is a relatively low contrast feature compared to real weld defects, such as undercuts or centerline cracks. The enigma can be distinguished from weld defects by these microdensitometer traces. The enigma effect on weld properties is not known but is expected to be minor.

ACKNOWLEDGEMENTS

This work was primarily of a survey nature but is dependent on the experimental work of Mr. E. O Bayless and his staff in experimentally simulating these features. It also benefitted from the information and inspiration of Dr Arthur C Nunes. Both are my counterparts. Any success is directly due to their guidance and cooperation.

It is my pleasure to acknowledge the assistance of several other individuals who helped me directly. They are Mr Carl Wood, who was totally sympathetic and supportive of my needs with respect to basic engineering information. Mr Paul H Schuerer inherited me into his branch with good grace and was very encouraging in his support. Messrs Paul Munafo, Bobby Rowe and Joe Montano offered constructive criticism. Claud Williamon and I worked together collecting x-ray data on fluorescence effects and Jim Coston was very helpful in analogous studies using the SEM. Dr Walter Fountain provided the critical bit of experimental evidence to confirm the basic ideas concerning the enigmas. Mr C Lovoy, USBI, retired NASA staff member has taken an interest in my activities and provided helpful background and information on several occasions. Several individuals of the Martin Marietta staff at Michoud were helpful in providing information. I am especially grateful to Messrs. Monty McAndrews and W. Mattheessen and to Ms Linda Johnston.

Introduction

There is an anomalous, generally linear feature in line with the weld direction that appears intermittently in weld x-ray radiographs. It bears an appearance similar to that of a defect, but for which there is no defect or discontinuity in the structure of the weld metal and no apparent effect on the weld mechanical properties. It is commonly called an *enigma* or *ghost defect*. Duren and Risch reported in 1970 (1) that: *The enigma is the most difficult discontinuity to determine, often being mistaken for incomplete fusion, and many times for a crack, or even a diffraction pattern. Identification of an enigma demands long experience in interpreting radiographs. The interpreter should notice that the dark line is always accompanied by a parallel light line. Many destructive tests for strength have been made of this type of discontinuity, but so far there has been no noticeable effect on the weld's ultimate strength.* This represents the understanding 15 years ago and indicates that the enigma must have been considered a problem for some time before that period. Welds of that time were not plasma arc, therefore the phenomenon is general.

Present indications are that there are two or more distinct manifestations of the enigma that occur separately. These are the dark form, frequently occurring along the weld centerline, and the gray or white line at the side of the weld, just within the fusion boundary. Real weld

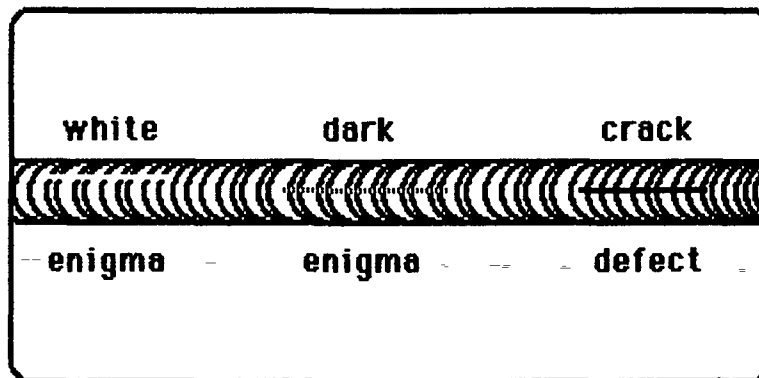


Figure 1. The typical appearance of enigmas and crack indications in a weld radiograph

defects are not a manifestation of the enigma. Both features, which have

been observed separately, have the appearance of a serious weld defect, but on close examination, by metallographic sectioning, have been found to be free of any defect. The problem is that the condition is misleading and disconcerting. The appearance is similar to that shown in Figure 1.

Recently, L. Johnston (2) reported that *the . . . enigma occurrence was characterized by a grey line running along the toe side of the weld. The line ran continuously, only occurring on one side at a time. No violations of weld parameters were found. The trim area was large enough for one tensile bar and one macro specimen. The UTS of the tensile bar was greater than 40 KSI. Visual examination of the weld revealed no cracks, undercut, suckback, open porosities or tunnels, or other evidences of inconsistent welding processes. No anomalies were found in ultrasonic inspection. Post-proof x-ray showed no change of character, position or intensity.* This report was corroborated by Kinchen and Brown (3).

The suggestion was made that the phenomenon is a diffraction effect, similar to Kikuchi lines in electron diffraction or Kossel lines in X-ray diffraction. Rummell and Gregory (4) reported a similar occurrence in radiographs of TIG welded 2014 aluminum alloy. *Recent studies on welding defects have revealed a phenomenon which appears as "lack of fusion" or "lack of penetration" in a weld radiograph, but does not affect the performance of the weld. . . indications are generally not as sharp as true lack of fusion, and are curved at the ends. . . Macro and micro examination of the weld cross section shows a dendritic grain structure in the fusion zone. . . Grain orientations are at right angles to each other. . . The unique grain orientation is due to a particular cooling and freezing process in the weld. . . Now, if a series of crystals are properly oriented with respect to an X-ray beam, a "focusing" effect will be observed on the radiograph, in the form of a dark band. . . The white line is caused by deviation of the transmitted beam by the diffraction process, thus decreasing the total transmitted radiation in a particular line or band. . . The diffraction process is not limited to the weld structure illustrated, but will occur in any exposure when crystalline planes are properly oriented with respect to the X-ray beam. Likewise, this process is not limited to aluminum welds.*

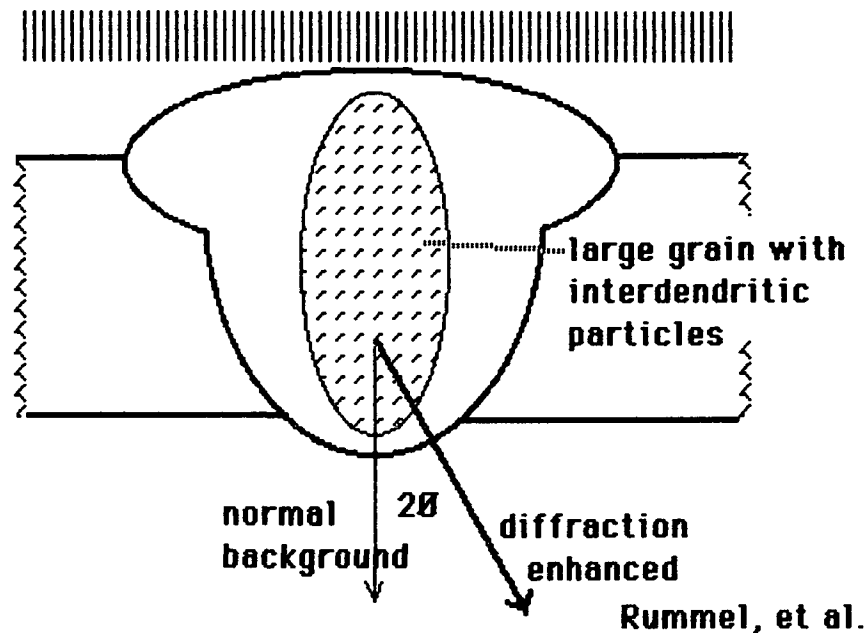


Figure 2. X-ray diffraction as a cause of the dark line weld radiograph enigma

Figure 2 illustrates the general features of the Rummell model. The interdentritic particles shield the film producing the light line and the diffracted beam produces the dark band. Large grains of this type are encountered occasionally. Since the solidification mode is generally dendritic and the interdentritic constituent is of an eutectic type the second phase particles are likely to be coherent, or at least highly aligned, with the dendritic branches. Finally, since the film is generally placed very close to the sample, the physical separation of the direct and diffracted beams on the film is also close.

Hirosawa et al. (5) reviewed the literature, including the work of Rummel et al. and Tucker et al., who reported similar findings and conclusions to those of Rummell (6). Rabkin et al. also reported dark band enigma formation in Al-Mg alloy welds (7). Issiki reported similar effects in aluminum alloy castings (8), and Irie, et al. reported similar features in stainless steel welds (9). Hirosawa et al. reported an analytical procedure related to magnesium content in aluminum alloys (5).

It is evident that the enigma, ghost defect or linear anomaly has been encountered for a number of years and in a number of alloy systems and welding processes. It appears to consist of dark or light lines, separately or together, primarily straight, in alignment with the welding direction, but also may have a curvature. The curvature is due to changing

conditions along the weld path. All reports place these features in the fusion zone. The dominant questions to be answered in finding the solution to the weld radiograph enigma problem are:

1. What is the enigma?
2. What produces the effect?
3. How can it be recognized?
4. How are weld properties affected?

The question about the effect on properties is fundamental. However, it must be realized that even if there is a visible feature in the sample there are established size tolerances. Perhaps the greatest problem is the inability to distinguish the enigma from a weld defect. A method was evaluated for this purpose and is described in a later section. There are many manifestations of the enigma. It will be shown to be a fine structure in the weld radiograph that is related to a real condition in the weld. The occurrence of this fine structure will be related to such factors as concentration gradients, shape effects and possibly features as severe as porosity. Even these latter, at levels to produce a visible feature, are probably within the established size tolerances. The correct interpretation of these features requires an understanding of the principles of welding physical metallurgy and image formation in x-ray radiography.

Experimental

The space shuttle external tank is fabricated, primarily, of aluminum alloy 2219-T87. The initial joining process was TIG welding which is being replaced by VPPA welding. The filler material is 2319 aluminum alloy wire. Weld radiograph enigmas were reported for TIG welds as well as the VPPA process. TIG weld radiographs show a higher level of density variation than VPPA radiographs, therefore fine structure is not as easily detected.

In most thicknesses, two weld passes are used, both from the same side. The root pass is in the keyhole mode and the cover pass in partial penetration, frequently referred to as "in the TIG mode." The plasma has a remarkable cleaning action. The heavy ions break up the tenacious oxide layer and the fragments are swept away by the plasma jet. If the

torch is properly aligned and the parameters properly set, a flawless weld results. Even the cover pass maintains the high level of structural integrity due to the action of the keyhole pass which leaves a clean system. The shape of the liquid puddle during the vertical up keyhole pass is shown in Figure 3.

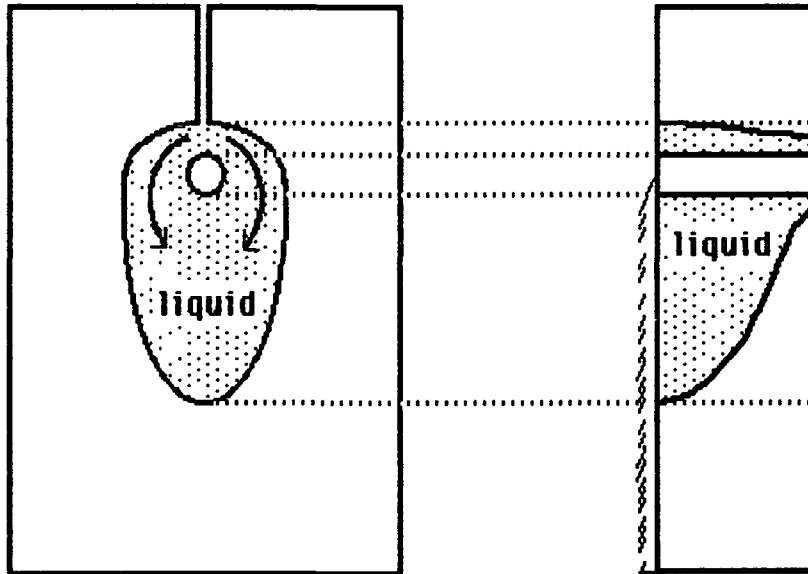


Figure 3. General shape of the keyhole mode weld pool.
The shaded portion is the liquid

The final weld structure is characterized by crown and root reinforcements making a smooth transition to the base metal plate on both surfaces. Figure 4 describes the general appearance of the weld after the root and cover passes. The root reinforcement is produced in the keyhole pass and the top surface of the weld is left approximately flush. Thinner plates are welded in only a single pass leaving reinforcements on both surfaces. The cover pass remelts a portion of the fusion zone of the previous keyhole pass and part of the base metal. The symmetry shown in the sketches of Figure 4 can be expected as the result of symmetric torch alignment. The heat affected zone exhibits only a minor change of grain size. The hardness profile across the weld from one base metal plate to the other shows a generally symmetrical decrease in hardness towards the weld centerline with a moderate increase close to the fusion boundary in the heat affected zone. This small increase is due to an age hardening effect.

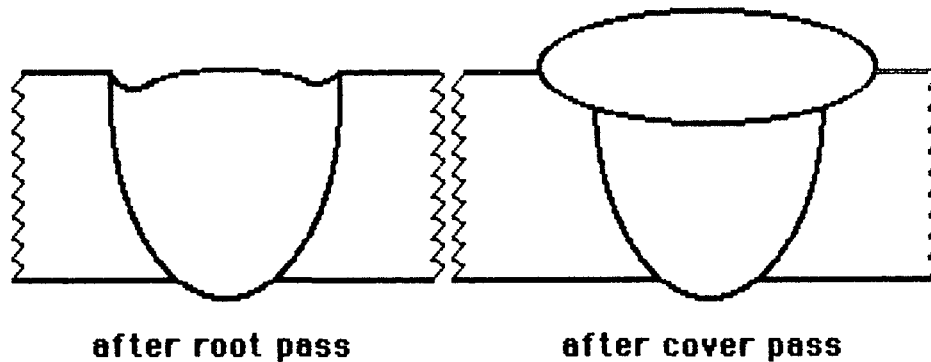


Figure 4 Shape of the weld after the root pass (left) and the cover pass (right) in VPPA welding

X-ray radiography uses a tungsten target tube operated at a tube voltage of 80 Kv and a tube current of 15 ma. The typical standoff distance is 40 inches. In most cases the film is placed in direct contact at the back of the sample. However, in one of the fixtures this space is restricted so that the film is approximately 1.25 inches away. The exposed film is processed automatically and is read and interpreted visually. Other NDE procedures are employed to clarify and decide specific conditions. Present practice requires 100% radiographic inspection.

Three densitometers were used to obtain line traces across the weld pattern. These are the MacBeth TD 102 densitometer with an aperture of approximately 3 mm diameter, an instrument which is designed for analyzing spectroscopic plates, and the Perkin Elmer PDS Microdensitometer developed for analyzing stellar plates. The Perkin Elmer instrument was operated with a square aperture of 125 μm side dimension at contiguous fields. An offset density of 1.5 was uniformly used for all measurements. The data was printed out and manually transferred to a personal computer for processing. The second instrument could not be used due to its inability to work with high density radiographs.

The scanning electron microscope with an EDAX chemical analysis attachment was used to map the concentration of copper and iron over transverse sections of the weld.

Radiography, based on the fluorescence of alloying elements, was used to map concentration distribution. In another investigation of fluorescence effects, the standard x-ray facility was operated at a standoff distance of 40 inches over a range of tube voltages. The film (DuPont

Cronex 45) was placed over blocks of pure copper and lead, placed side by side. The exposure was controlled by setting tube current, exposure time and using various thicknesses of 5052 aluminum alloy plate

Contributing Factors

Welding:

Welding exerts its influence on the condition of the final solid through all of its operating parameters. Conditions in the liquid pool control weld geometry, grain shapes and final distortion and residual stresses. The hot, just solidified alloy behind the pool, contracts as it cools, whereas the base metal away from the weld may not have any tendency to contract. If the effective center of this initially hot metal is out of line with the center of mass of the plate, the contraction produces a net bend and leave a serious pattern of residual stresses as shown in Figure 5, which illustrates the directions of these distortions. This is explained in detail by Masubuchi (10). These stresses, in concert with applied stresses can lead to premature service failure. If a stress riser, or other mechanically sensitive feature is in the field of influence of the stress pattern, cracking can occur.

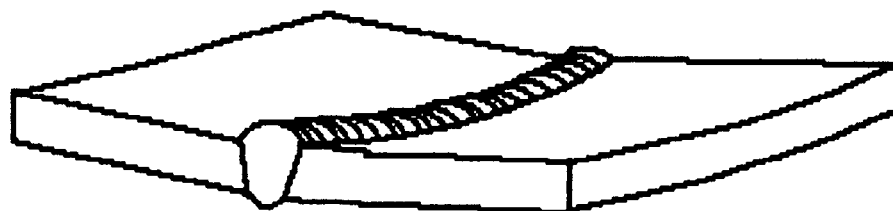


Figure 5. Shrinkage distortion in a butt weld. This distortion includes peaking and longitudinal curvature.

Fixturing can be used to control or reduce distortion. It also exerts an effect on the final microstructure by alteration of the heat sink configuration. This modifies the pattern of grain growth and affects

properties. The effect on grain growth direction is illustrated in Figure 6. In a previous study (11) the application of cooling blocks along a short region at the side of the weld produced a finer microstructure and increased the mechanical properties in that section.

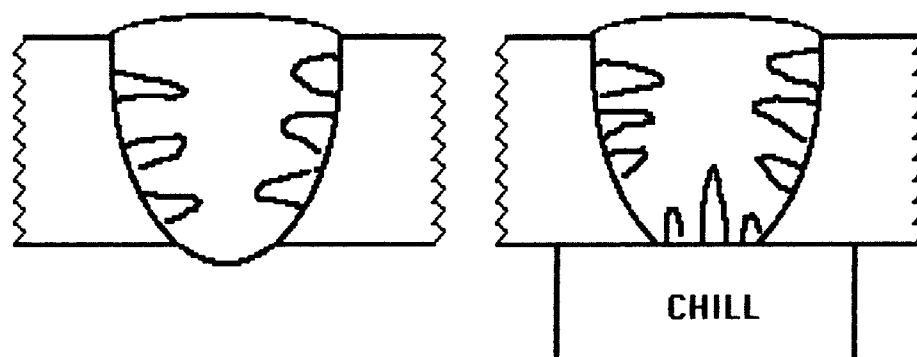


Figure 6. The effect of heat sink configuration on the weld metal grain structure

Welding power and speed affect the final weld structure through their action on final cooling rate. Power must, of course, be set to control penetration and width. The higher the speed the more power is required to penetrate to the proper depth. At higher welding speeds the base metal is not heated to the same extent and has a greater cooling effect after the torch passes. This changes weld shape and affects the direction of heat flow. The desired ellipsoidal shape of the weld pool becomes pointed at the back as illustrated in Figure 7. The consequence is that the direction of columnar grain growth in the fusion zone is affected. If the condition is sufficiently pronounced a plane of weakness is formed along the weld centerline. Cooling stresses may then result in centerline cracking.

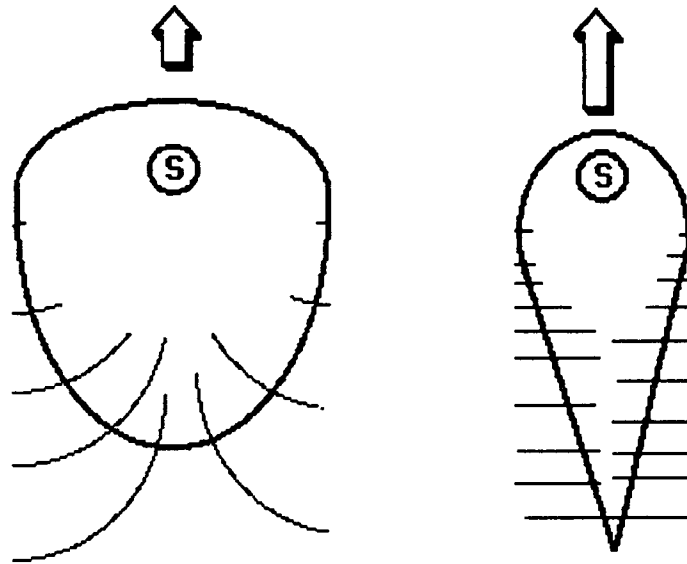


Figure 7 The effect of welding speed on shape of the fusion zone and weld metal microstructure. The relative lengths of the arrows represent welding speed.

At the other extreme of welding speed the final fusion zone structure will be too coarse due to the slow cooling conditions supported by the well heated base plate. Coarse microstructure is associated with lower mechanical properties. In a previous research it was shown that an increase in interdendritic particle size from 10 to 150 μm correlates with a 10 ksi decrease in weld tensile strength (11). The effect of welding speed in electron beam welding is dramatically illustrated in a brief review note by Komizo, et al. (12). These same effects are also characteristic of any moving source fusion welding process, such as VPPA welding.

Weld metal morphology, which is primarily dendritic, is controlled by the solidification process. Grains have columnar shapes directed along the line of heat transfer. For a given materials system welding speed has the greatest influence on the grain shapes and directional pattern in the fusion zone as well as the size of the structural features. The secondary dendrite branch dimension is the critical size parameter in the fusion zone microstructure. The product of welding speed and the square of the size parameter is a constant for a given materials system and solidification process.

Stresses are developed by differential cooling from a

condition where pronounced temperature differences exist within the system. Under these conditions any possible stresses are released due to the enhanced plasticity at the elevated temperature. As the hot metal cools, its strength increases and its contraction, relative to the condition of the initially cool metal causes locked-in stresses to develop. The magnitude and direction of these stresses is influenced to a lesser degree by variations in solidification conditions.

Solidification:

Solidification is the most significant process in weld metal structure and properties. The basic weld characteristics that are directly affected include.

- 1 chemical segregation
- 2 second phase production
- 3 porosity

It is not possible to remove solidification factors from welding process factors since they are totally interdependent. They must be considered together in any given application. However, selected topics in the physical metallurgy of weld metal solidification will now be considered.

Chemical segregation is a dominant factor and can be readily explained in relation to the aluminum-copper phase diagram, which applies to the 2219 alloy. The nominal copper composition is 6.3% by weight. Reference to the diagram shows that the composition line is to the right of the maximum solid solubility point of 5.62% copper (548 °C). Therefore it can be expected that there will be free particles of CuAl_2 intermetallic compound in the microstructure, regardless of the treatment after solidification. Under steady state welding, the weld pool composition corresponds to this same 6.3% Cu value.

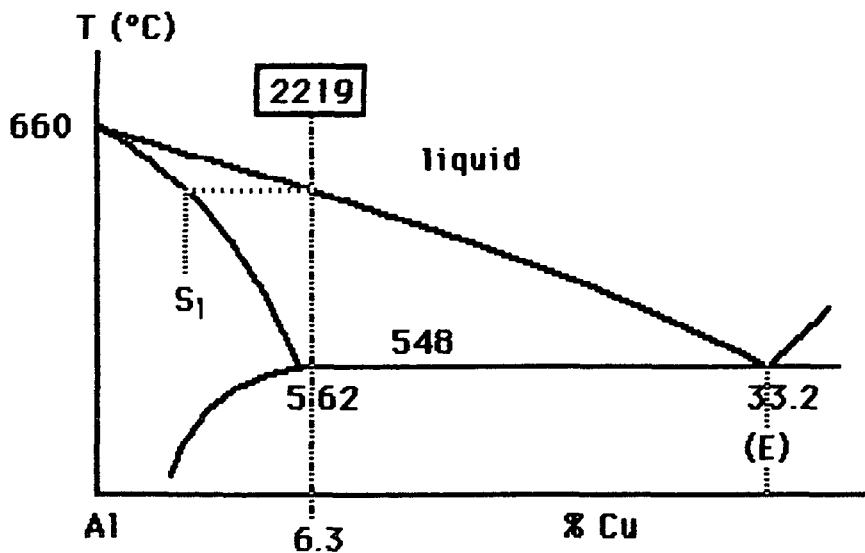


Figure 8. Aluminum rich end of the Al-Cu phase diagram. The composition of 2219 aluminum alloy and the solid that forms initially are shown. The eutectic constituent, (E), is a coherent mixture of aluminum solid solution and CuAl_2 intermetallic compound.

The composition of the first solid to form on cooling is S_1 (marked on the diagram) and is formed at a temperature of 640 °C. As solidification continues, the copper, that is not incorporated in the first solid, enriches the liquid so that it freezes out at a lower temperature, corresponding to a further position along the solidus line. The last solid to form is an eutectic mixture, with a composition of 33.2% copper. It freezes at 548 °C. It is this liquid that contains the highest copper content and is most likely to flow against the coolest surfaces of the cooling weld. It has the greatest capacity to fill any cracks or other openings in the weld metal.

The solid-liquid boundary surface of the weld pool is not isothermal but varies from a temperature corresponding to the freezing temperature of S_1 at the positions where solidification commences and drops to the eutectic solidification temperature at positions directly behind the moving source.

Second phase production is an important aspect of solidification. In this alloy system the second phase can be formed in two constituents. The intermetallic compound phase (53% Cu) is formed in either the fusion zone or heat affected zone and is in the parent metal.

microstructure. The second constituent, the eutectic mixture is only in the fusion zone - a product of solidification. It is this constituent that is important in some forms of enigma and this is a major controlling factor on the weld tensile strength. It does not influence the yield strength very strongly since this property is dominated by the solid solution that comprises most of the microstructure.

Bayless (13) produced weld structures to demonstrate the light line enigma. His method involved the intentional misalignment of the torch for the root pass, thus producing a deep undercut to one side of the weld and an exaggerated buildup of metal to the other side. The normal and misaligned final profiles are shown in Figure 9.

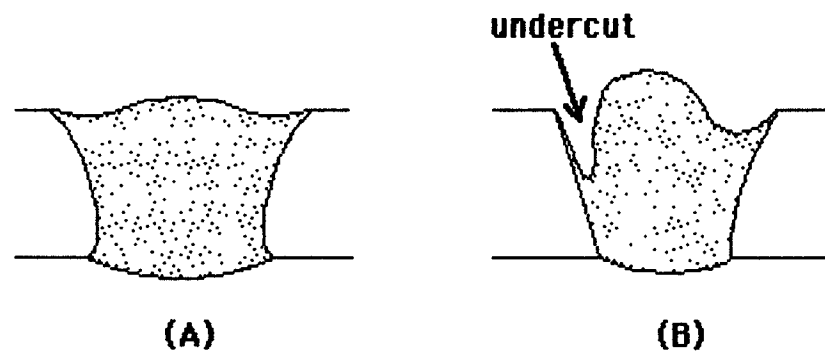


Figure 9 The shapes of the desired (left) and misaligned (right) shapes of the root pass weld metal.

When the cover pass was applied, the final structure showed the enigma due to the concentration of eutectic mixture in the undercut. The cover pass only partly repaired the initial improper shape. The deepest part of the undercut, which was not remelted was filled with eutectic liquid during welding. This left a residual copper-rich band of the form described above in the enigma simulations. The first three microdensitometer traces were made on the radiographs of the Bayless simulation samples. Lancaster discusses other methods to cause these effects (14).

Porosity is a type of second phase that results from solidification. There are several causes including.

1. The release of gases dissolved in the liquid.
2. The entrapment and release of hydrogen that is

produced by the decomposition of water or hydrocarbons left on the surface of the metal or filler wire prior to welding

- 3 The failure to fill the interdendritic regions due to insufficient eutectic liquid
- 4 The freezing over of interdendritic regions, thus preventing access by the available eutectic liquid

The first two sources produce a more uniform distribution of porosity throughout the new solid but the latter two develop concentrated openings in the vicinity of the center line. None of these are typical of VPPA welding of 2219-T87 aluminum alloy. See Easterling (15) for more information about porosity in welding.

Radiography:

The initial x-ray beam is directed normal to the principal plane of the sample and is uniform in intensity. This uniformity is achieved by employing a long distance between source and film.

Passage through the sample reduces the intensity of the entire spectrum in proportion to the sample thickness and its absorption characteristics, which are a function of wavelength. The beam is further attenuated as it passes through the film. The energy lost in the sample produces the pattern seen in the film after it is developed. The radiation absorbed in the film causes the darkening. The thinner the sample, the more radiation penetrates to reach the film, and the more particles of silver that are developed in the emulsion to darken the film.

These features are represented in Figure 10. The thickness of the lines representing the x-ray beam, that is moving downwards, indicate the relative intensities. The points in the film cross section represent particles of silver, after development. The effect of the reinforcement is to increase the absorption and reduce the final silver content in the corresponding parts of the film.

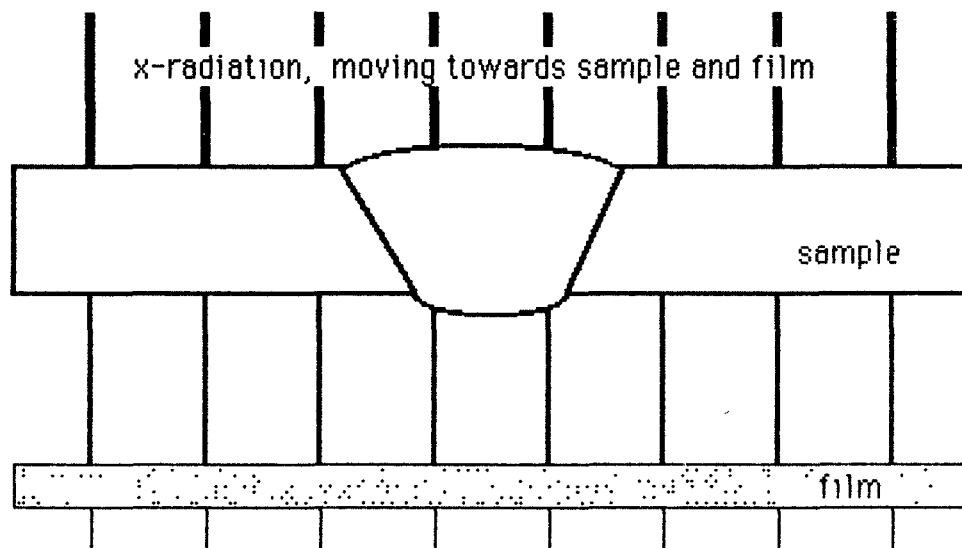


Figure 10. Representation of the general configuration for the preparation of an x-ray weld radiograph. The distance between the sample and film is exaggerated in this figure.

The physical processes involved are outlined in figures 11 and 12. See Cullitty for a comprehensive presentation (16). The spectrum of the initial beam is shown in the first block at the left of figure 11. The spectrum of the final beam is shown at the right. Under the typical 80 Kv tube operating conditions, spectral content of the initial radiation is primarily a continuous distribution of x-rays, generally identified as *continuous, white or brehmsstrahlung*. A characteristic of tungsten and other high atomic number target material tubes is the suppression of characteristic radiation peaks. There probably is a small component of characteristic K_{α} or K_{β} radiation. Such a peak is shown schematically. There is only a small energy content in these characteristic radiation components.

After passage through the sample the intensity of radiation is generally diminished, as shown in the block diagram to the right. This attenuation is most pronounced in the vicinity of the absorption edge of the important chemical components in the sample. The relationship between thickness, materials characteristics and initial and reduced intensities is written below the sample.

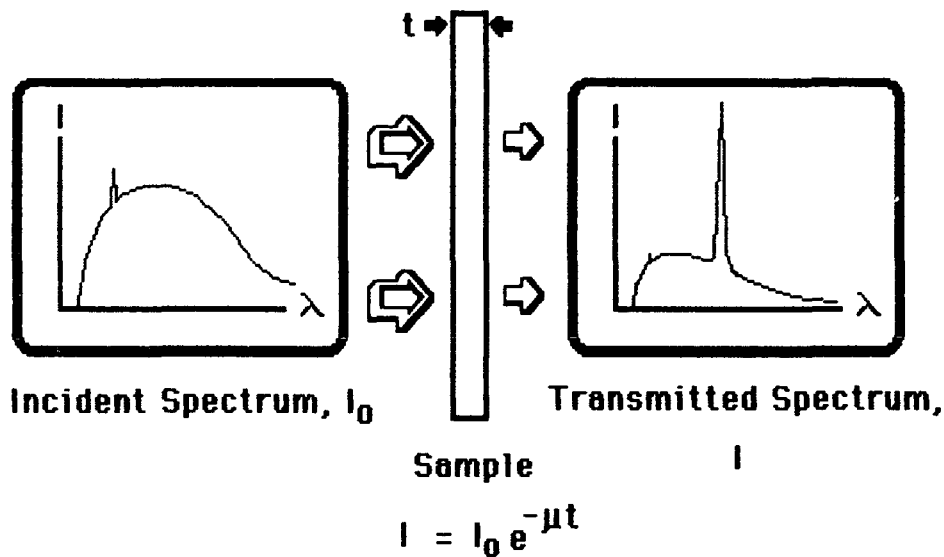


Figure 11 The spectrums of the initial and transmitted x-ray beams in radiography

Each element has characteristic absorption characteristics in the form shown in Figure 12. Energy is absorbed when specific electronic processes are induced within the elements of the sample. The energy invested in these processes can be recovered in different ways. Copper, for example, has an absorption edge at 1.38059 Å and uses this energy to produce fluorescent radiation of 1.54 Å wavelength. In this case, the characteristic radiation is added to the spectrum. These processes are most active when there is energy at the lower wavelength side of the absorption edge. In this case, the sample acts as a source of *secondary radiation*. This usually has the undesirable effect of increasing the general background density of the film and tending to obscure the features of the image.

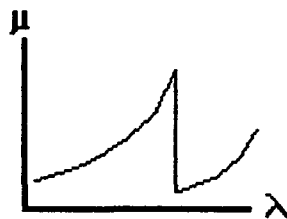


Figure 12. Typical absorption curve.

Diffraction is a possible contributing factor because diffraction can cause extra radiant energy to be concentrated along specific directions. Rummell referred to one specific diffraction effect. Another, that has been mentioned, and should be considered is the development of Kossell lines, which are a phenomenon in the class of wide angle scattering (17-19). If the linear anomaly in the radiograph is actually due to a diffraction effect, the features will be characteristic of that effect and can be recognized by appearance.

In one application, the Kossell pattern is developed by placing a thin layer of fluorescent material, such as copper, against the side of the single crystal sample that is towards the source. When the narrow beam of x-rays strikes the sample this layer then provides an x-ray source at that close location to produce divergent diffracted beams. These rays are contained within a conical surface, intersecting the film in arcs. This type of enigma structure has not been reported.

Anomalous transmission, known as the Borrmann effect (20-23), can also make a contribution to the intensity of x-rays delivered to alloying elements concentrated close to the film within the weld. The necessary conditions are a large, favorably oriented grain of a single crystal phase. Such large grains have been observed in weld metal. They are formed due to the maintenance of conditions favoring stable growth, as opposed to nucleation. These conditions include a favorable alignment of a high symmetry crystal direction with the vertical, along which the x-ray beam propagates. In aluminum, as is typical of most alloy systems, the favored growth direction is $\langle 100 \rangle$ which has the highest symmetry. There is a greater likelihood that for a grain that grows in a $\langle 100 \rangle$ direction parallel to the weld surface that it will also have another $\langle 100 \rangle$ type direction aligned vertically. Such an alignment would be naturally favored and would tend to prevent the growth of grains of other alignments. The formation of large, highly aligned grains should be no surprise in a solidification process as controlled as that in a VPPA fusion zone.

The natural conclusion is that a number of different factors contribute to the variation of radiographic film density across the weld. A number of these are summarized in Table 1 with respect to the direction of the darkening effect of each.

**Table 1
ABSORPTION**

FACTOR	DARKENING
Shape and Thickness	↓
Macro Openings	↑
Chemical Accumulation	↓ (Cu in 2219 Al)
Porosity	↑
Fluorescence	↑
Diffraction	↑ (possibly with ↓)
Anomalous Transmission	↑

It was found that persons can unambiguously distinguish adjacent light and dark areas when the density difference is only 1% (e.g. 2.98 and 3.01). The significance is that many features are observed that are only of secondary significance.

Results and Discussion

The above factors can produce a complicated visual pattern when combined. The following are microdensitometer traces made across welded panels of 2219-T87 aluminum plate. Figure 13 is a trace across the VPPA root pass made under conditions representing one set of torch alignment conditions marking the limit of acceptable practice. These traces are plots of data taken at a spacing of 125 μm along a line across the weld radiograph. There are 204 points per inch. The sample surface conforms to the desired shape, but the effect of the misalignment is visually obvious as is the lack of symmetry in the trace about the weld centerline. There is a minor degree of undercut along both edges of the weld (see 1 and 2). The undercut at 2 is more pronounced and wider. The peak at 3 corresponds to a

surface marking that runs along the side of the root reinforcement



Figure 13 Microdensitometer trace across radiograph of nearly symmetric root pass in a VPPA weld

Figure 14 is a similar trace across another unfinished weld (root pass only) made in the same plate. However, the torch misalignment

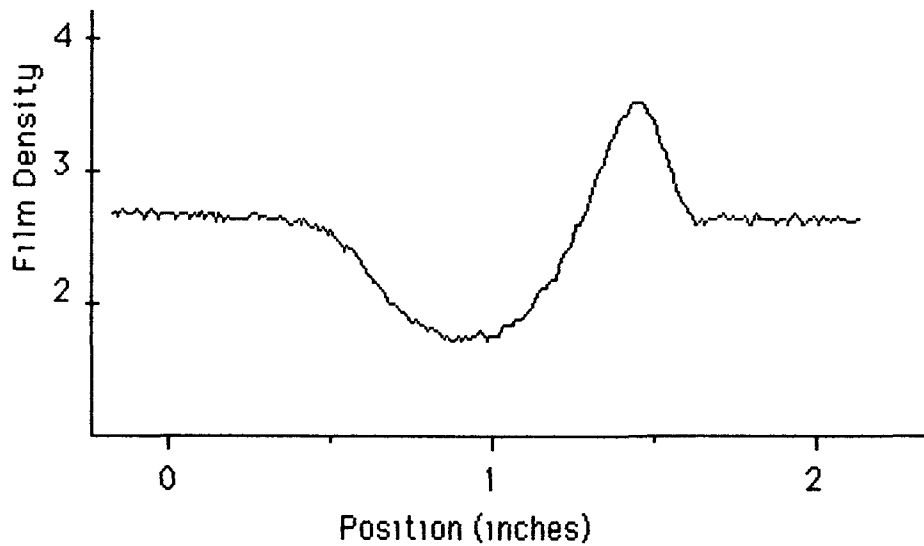


Figure 14. Microdensitometer trace across radiograph of root pass made under conditions of severe torch misalignment

was intentionally set to produce an extreme undercut along one edge. This is represented by the pronounced peak at the right. The deep valley at the left represents the region where the weld metal accumulated. This trace provides a good representation of the weld profile.

Figure 15 is across another weld made in the same plate, under the same conditions of misalignment, but with the cover pass applied. Even here the misalignment is detectable in the microdensitometer profile, although it is not visually detectable on the finished weld. Features 4 and 5 correspond with a weld root marking (see 1 in the first trace) and a surface scratch on the underside of the plate.

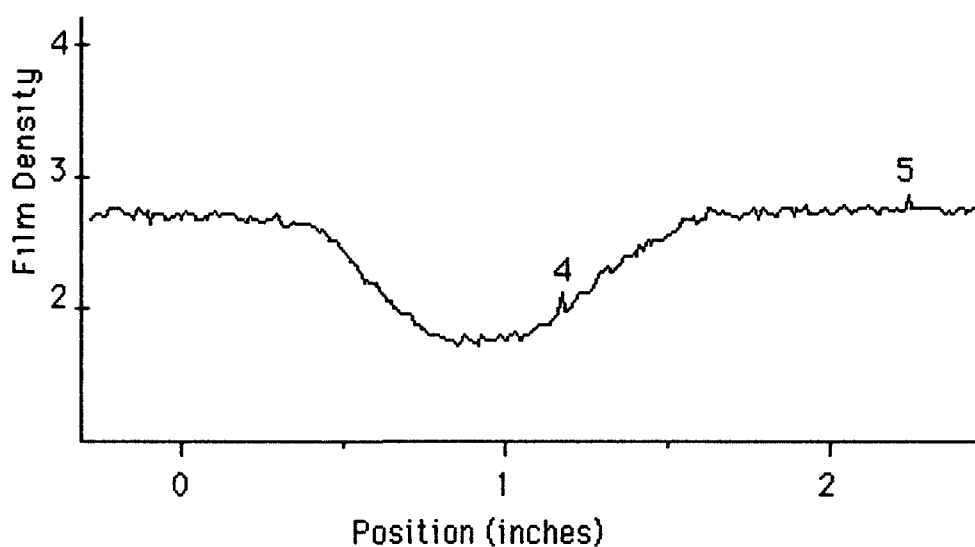


Figure 15 Microdensitometer trace of weld radiograph with cover pass over a misaligned root pass.

Figure 16 is a trace across a production radiograph showing two light line enigmas (marked 6 and 7). The appearance of the radiograph matches the appearance of the radiograph of Figure 15. The sample is not available.

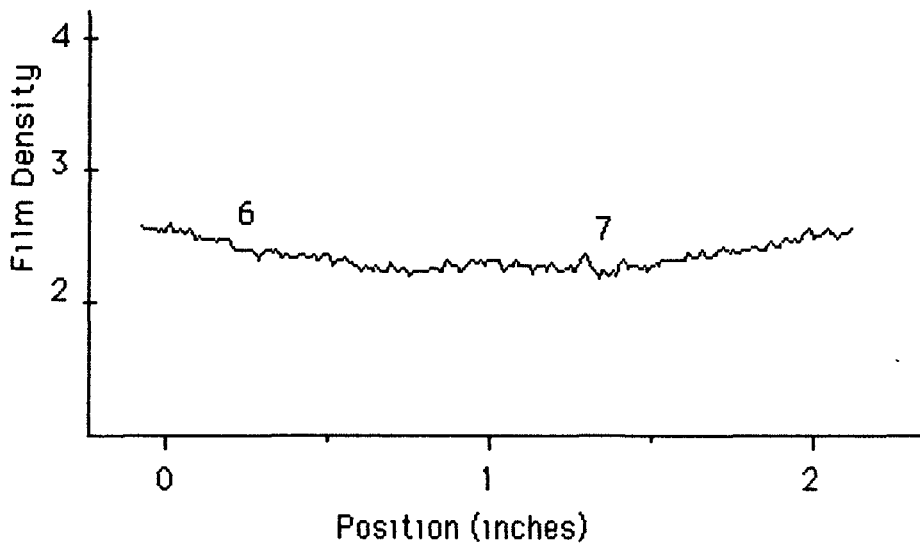


Figure 16 Microdensitometer trace across production weld radiograph

There is considerable detail, or *fine structure*, in the trace. These features can be related to the factors listed in Table 1.

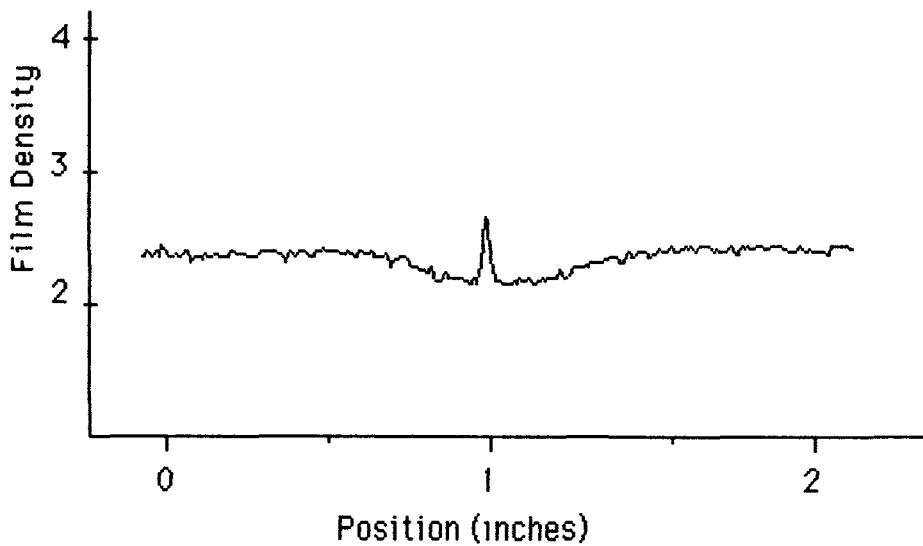


Figure 17. Microdensitometer trace across center line crack TIG welded 2219 alloy.

Figure 17 displays a trace made across the radiograph of a

TIG welded 2219-T87 plate with a definite centerline end crack. The appearance of the crack feature in the radiograph is very similar to the dark line enigma with the difference that the darkening associated with the real crack is much stronger in intensity.

Table 2 summarizes the density differences of the features noted in the microdensitometer traces.

TABLE 2
THE EFFECT OF ENIGMAS AND CRACKS
ON RADIOGRAPHIC FILM DENSITY

SAMPLE AND FEATURE	TYPE	DENSITY INCREMENT
Fig 13, feature 1	light	0.09
Fig 13, feature 2	light	0.05
Fig 13, feature 3	dark	0.05
Fig 14, total	shape	1.81
Fig 15, feature 4	dark	0.18
Fig 15, feature 5	dark	0.10
Fig 16, feature 6	light	0.13
Fig. 16, feature 7	dark	0.18
Fig 17, crack	defect	0.50

A series of measurements were made to evaluate the possible contribution of fluorescence. The film was placed over a composite background, with copper to one side and lead the other. The density of the resulting film was measured at five points within each field and averaged. The results are plotted in Figure 18 as darkening ratio versus tube voltage. At low voltages the copper produces a greater darkening, but this changes pronouncedly at a voltage between 80 and 120 Kv. The L absorption edge for lead is 0.95073 \AA , which indicates a critical wavelength just longer than 130 Kv. The nearest edge for copper is activated most effectively at tube voltages of 8900 v and slightly higher.

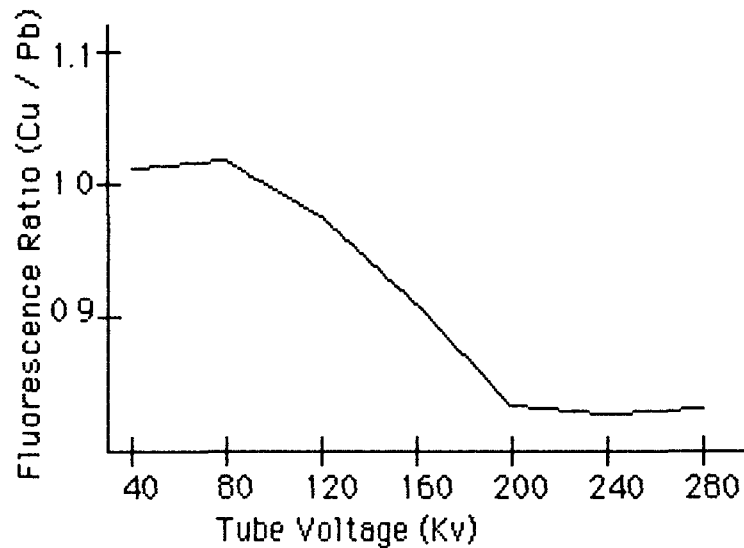


Figure 18 Ratio of backscatter over Cu to backscatter over Pb as a function of tube voltage

Along with these measurements, a radiograph was made of a large grained pure aluminum sample. This showed a general pattern of detail corresponding to the grain structure, although none of the grains is separately identifiable. This is evidence of the possible contribution of diffraction or anomalous transmission.

Enigma Simulation:

It is possible to simulate enigma formation. This is done by calculating the transmission ratio, I/I_0 , through the plate at each position across the weld. The basis of the calculation is Lambert's Law, $I = I_0 e^{-\mu x}$. In these equations, I is the intensity of the transmitted radiation and I_0 its initial intensity on the front side of the sample. e is the base of the Napierian logarithms, μ the absorption factor and x the distance of transmission through the plate. Since human sensitivity relates to $\ln I$, this response is directly represented by the magnitude of the exponential quantity, μx . Absorption is a characteristic of each chemical species and a function of wavelength. The values are generally available, usually listed as the mass absorption coefficient, μ/ρ , where ρ is the density. Thus response is measured by the product, $(\mu/\rho)\rho x$. In any mixture, the net mass

absorption coefficient is the linear average of the values for the elements, in proportion to their weight fractions in the mixture

Figures 19-21 are density traces generated in this way through the sample. In each figure, the sample is shown above and the film density representation directly below. It can be seen how the pattern of complexity in the radiographic film develops with the inclusion of complexity in sample shape and chemical segregation. This illustrates the origin of the enigma as well as the feasibility of simulating and interpreting these effects

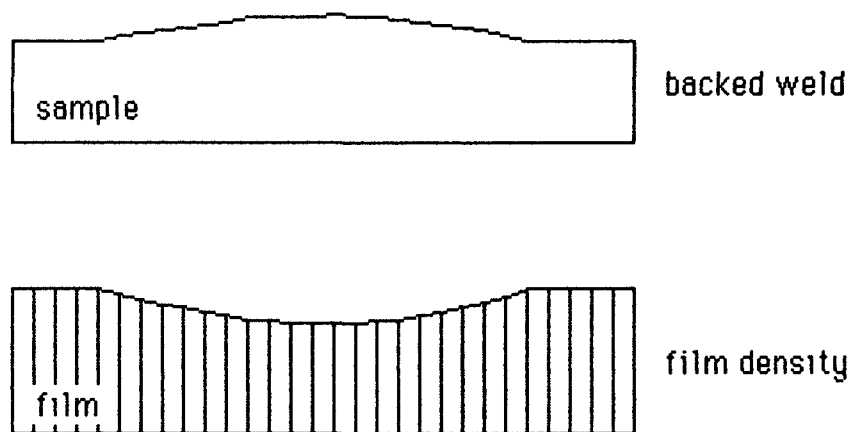


Figure 19. Computed film density for the sample shape shown.

Note that in this plot the density of the radiograph does not vary across the ends and has a curvature that matches the sample curvature. The sample shape corresponds closely to that of an actual weld, but the outline was drawn freehand on graph paper. The dimensions were read directly from this drawing and entered into the computer for the calculation. The result of the calculation was plotted and processed in a similar manner to that used for Figures 13-17. The variation in film density represented by the thickness of the cross hatched section is exaggerated several times.

The addition of the root reinforcement adds a bit of detail to the film density profile. The width of each reinforcement is clearly displayed in Figure 20.

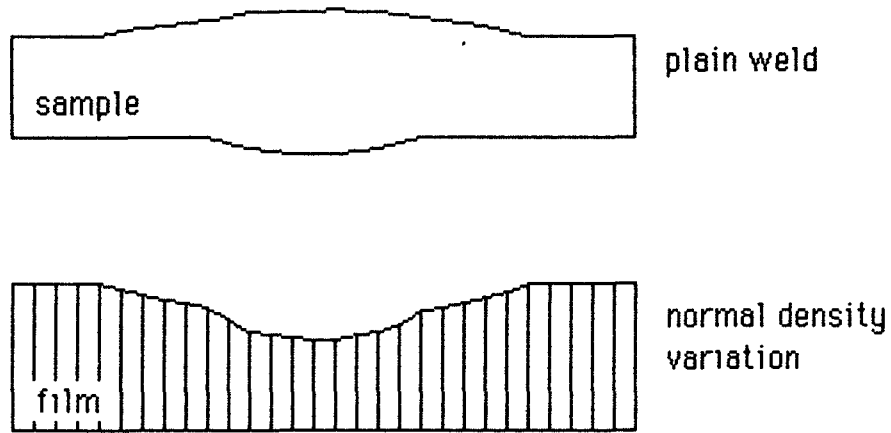


Figure 20. Film density variation across weld with both crown and root reinforcements.

Figure 21 was generated from the same weld configuration with an arbitrary addition of eutectic mixture. The angle of the deposit cross section, shown in the weld cross section, its thickness (0.5 mm) and the effective mass absorption coefficient, are reasonably close to experimental values, but are used primarily for illustration. The result is exaggerated.

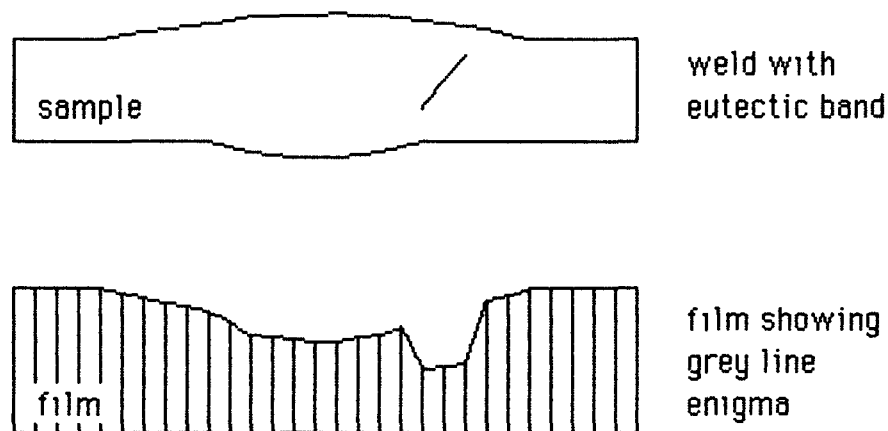


Figure 21. Computer simulated radiograph density across a weld with both reinforcements and a longitudinal band of eutectic mixture.

The grey line enigma of Figure 21 corresponds to that demonstrated by Bayless

Conclusions

The enigma is fine structure in the x-ray radiograph representing a real condition in the weld metal. There are many types of weld radiograph enigmas. The microdensitometer traces show that some features of radiograph fine structure can be related to visible features on the weld. The correspondence between radiograph fine structure and weld metal condition awaits direct verification, although the present indications are promising. The microdensitometer trace method can be used to reconcile these features of weld radiographs. Initial measurements indicate that the enigma represents a density difference of the order of 0.1 and that the crack defect represents a difference of the order of 0.5. It is suggested that this method be developed for weld evaluation and possible in-process control.

Weld radiograph fine structure is generally aligned in the welding direction, hence when it is sufficiently pronounced it is classed as a linear anomaly, or enigma. Changing conditions along the weld can produce a general curvature, which can explain curved enigma features. The full effect on properties is not known. The enigma cannot be eliminated and is not a feature of VPPA welding alone - it is a general phenomenon.

Bibliography

1. P. C. Duren and E. R. Risch, "Radiographic Interpretation Guide for Aluminum Alloy Welds," *NASA Technical Memorandum NASA TM X-53939*, (May 19, 1970), page 8.
2. L. Johnston, "VPPA 'black line' Anomaly Indication on X-Ray Films," Memo for the Record, August 21, 1984.
3. Kinchen and Brown; "Evaluation of VPPA Radiographic Anomalies in 2219 Aluminum Weldments," Laboratory Test Report, Metallurgical Analysis, 85A205, (6-3-85).
4. W. D. Rummell and B. E. Gregory, "'Ghost Lack of Fusion' in Aluminum Alloy Butt Fusion Welds," *Materials Evaluation*, *XXIII*, (1965), 586.
5. E. Hirose, M. Naoe and T. Fukui, "'Ghost Defects' In Radiographs of

- Aluminum Alloy Welds," *Materials Evaluation*, *XXIX*, (1971), 99.
- 6 M. S. Tucker and P. A. Larssen, "Markings in Radiographs of 2014 Aluminum Alloy Gas Tungsten-Arc Welds," *Welding Journal*, *47*, (1968), 223
 - 7 D. M. Rabkin, L. A. Bukalo, V. Ta. Kirzhova and A. S. Deniyanchuck, "Weld Heterogeneity in Aluminium-Magnesium Alloys," *Avt. Svarka*, No 5, (1966), 74
 8. S. Issıki, J. Ko, K. Kataoka and T. Yamazawa, "The abnormal Pattern in Radiographs of Aluminum Alloy Castings," *Hihakai-Kensa*, *15*, (1966), 257
 - 9 M. Irie, M. Fujii and S. Yamashita, "The Influence of Structure on the X-ray Radiograph of Stainless Steel Welds," *Hihakai-Kensa*, *12*, (1963), 263
 - 10 K. Masubuchi, "Residual Stresses and Distortion, Chapter 6," *Welding Handbook*, *1*, 7th Edition, American Welding Society, (1981), 223
 - 11 W. A. Jemian, "The Strength and Characteristics of VPPA Welded 2219-T87 Aluminum Alloy," Final Report, NASA-ASEE Summer Research, (1984)
 - 12 Y. Komizo, C. S. Punshon, T. G. Gooch and P. J. Blakely, "Effect of process parameters on centre line solidification structures of electron beam welds in steel," Welding Institute Members Report No 252, (1984)
 - 13 E. O. Bayless, personal communication
 14. J. F. Lancaster, *The Physics of Welding*, Pergamon, (1984).
 - 15 K. Easterling, *Introduction to the Physical Metallurgy of Welding*, Butterworths, (1983).
 - 16 B. D. Cullitty, *Elements of X-Ray Diffraction*, Addison-Wesley, (1978).
 17. A. Taylor, *X-ray Metallography*, Wiley, (1961), 770

18. L. S. Birks, *Electron Probe Microanalysis*, 2nd Edition, (1971), 140.
19. H. Yakowitz, "The Divergent Beam X-Ray Technique," *Electron Probe Microanalysis*, Academic Press, (1969), 361.
20. G. Borrmann, "Röntgenwellenfelder," *Trends in Atomic Physics*, Risch, Paneth, Roosbaud, Editors, Interscience, (1959), 262
21. L. P. Hunter, "X-Ray Measurement of Microstrains in Germanium Single Crystals," *J. Appl. Phys.*, 30, No. 6, (1959), 874
22. B. W. Batterman, "Imaginary Part of X-Ray Scattering Factor for Germanium Comparison of Theory and Experiment," *J. Appl. Phys.*, 30, No. 5, (1959), 998.
23. A. Guinier, "Small Angle X-Ray Conference Proceedings," *J. Appl. Phys.*, 30, No. 5, (1959), 601